Indian Journal of Engineering & Materials Sciences
Vol. 19, February 2012, pp. 47-53

Electrical conductivity of Ca-doped $YFeO_3$

K T Jacob[a]*, G Rajitha[a] & N Dasgupta[b]

[a]Department of Materials Engineering, Indian Institute of Science, Bangalore 560 012, India

[b]Department of Materials Science and Engineering, University of Utah, Salt Lake City, UT-84112-5630, USA

Received 28 September 2010; accepted 24 February 2012

Electrical conductivity and Seebeck coefficient of calcium-doped $YFeO_3$, a potential cathode material in solid oxide fuel cells (SOFC), are measured as function of temperature and composition in air to resolve conflicts in the literature both on the nature of conduction (*n*- or *p*-type) and the types of defects (majority and the minority) present. Compositions of $Y_{1-x}Ca_xFeO_{3-\delta}$ with x = 0.0, 0.025, 0.05 and 0.1 are studied in the temperature range from 625 to 1250 K. All $Y_{1-x}Ca_xFeO_{3-\delta}$ samples show *p*-type semiconducting behaviour. Addition of Ca up to 5% dramatically increases the conductivity of $YFeO_3$; increase is more gradual up to 10%. A second phase $Ca_2Fe_2O_5$ appears in the microstructure for Ca concentrations in excess of 11%.

Keywords: $Y_{1-x}Ca_xFeO_{3-\delta}$, Ca-doped yttrium ferrite, DC electrical conductivity, Seebeck coefficient, Activation energy

The calcium-substituted orthorhombic perovskite yttrium orthoferrite ($YFeO_3$) with the space group *Pbnm*[1] appears to be a candidate for cathode material in solid oxide fuel cells (SOFC) based on its electrical conductivity. Because of better size compatibility, Ca^{2+} substitutes on the Y^{3+} site leading to the formula $Y_{1-x}Ca_xFeO_{3-\delta}$. To understand the conductivity mechanism, Yoo and Kim[2] studied the four-probe DC electrical conductivity and thermoelectric power of $Y_{1-x}Ca_xFeO_{3-\delta}$ (YCF) samples as a function of composition, temperature and ambient oxygen partial pressure in ranges of $0.0 \le x \le 0.7$, $300 \le T/\mathrm{K} \le 1373$ and $10^{-16} \le P_{O_2}/\mathrm{P^o} \le 1$ (where P^o is the standard atmospheric pressure 1.013×10^5 Pa), respectively. They observed that the solubility limit of CaO in the orthoferrite occurs at $x \approx 0.1$ and addition of Ca enhances the conductivity of $YFeO_3$ enormously. YCF was identified as a *p*-type conductor in air at all temperatures, but changes from *p*-type to *n*-type with decreasing oxygen partial pressure. A small polaron hopping mechanism with a hopping energy of 0.15 to 0.19 eV for $x \neq 0$ was proposed. In a later study Kim and Yoo[3] observed small oxygen ion conductivity in $Y_{0.9}Ca_{0.1}FeO_{3-\delta}$ with transference number in the range from 10^{-4} to 10^{-2} depending on oxygen partial pressure. The activation energy of 1.6 eV is associated with oxygen ion conductivity in the temperature range $1173 \le T/\mathrm{K} \le 1373$ for oxygen partial pressures in the range $10^{-16} \le P_{O_2}/\mathrm{P^o} \le 1$. Contrary to these early studies, Cao *et al.*[4] reported intrinsic *n*-type conduction in pure $YFeO_3$ based on negative values of Seebeck coefficient and increase in conductivity with decreasing oxygen partial pressure. The main focus of Cao *et al.*[4] was the investigation of the effect of Mn substitution for Fe in $YFeO_3$. Liu *et al.*[5] confirmed the enhancement of the conductivity of $YFeO_3$ by Ca doping in samples prepared by gelcasting. They reported hole-hopping activation energy of 0.445 eV and 0.148 eV for pure $YFeO_3$ and $Y_{0.9}Ca_{0.1}FeO_{3-\delta}$ after sintering at 1523 K. The activation energy for $Y_{0.9}Ca_{0.1}FeO_{3-\delta}$ changes to 0.131 eV after sintering at 1573 K because of reduced porosity. The experimental methods used by different investigators[2-5] and defect structures identified for doped and undoped $YFeO_3$ are summarized in Table 1. To resolve discrepancies in the literature on the nature of conduction (*n*- or *p*-type) and the defects present (majority and the minority) the electrical conductivity and Seebeck coefficient were redetermined in this study as a function of concentration of Ca dopant and temperature. In a recent phase diagram study of the system CaO-Fe_2O_3-Y_2O_3 at 1273 K in air, the solubility limit of CaO in $YFeO_3$ was found to be 11 mol %, corresponding to a value of x = 0.11 in $Y_{1-x}Ca_xFeO_{3-\delta}$.[6] The phase that forms at higher

*Corresponding author (E-mail: katob@materials.iisc.ernet.in)

Table 1—Defect structure for $Y_{1-x}Ca_xFeO_{3-\delta}$

Investigators	Techniques Used	Defects	
		$x = 0$	$x > 0$
Yoo & Kim[2]	Four probe DC conductivity and thermoelectric power as a function of P_{O_2} and T.	Disproportionation of Fe^{3+}: $2Fe_{Fe}^{X} \Leftrightarrow Fe_{Fe}^{\bullet} + Fe_{Fe}^{'}$ (enthalpy = 2.4 eV); p-type: $\mu_n \approx 0.2\mu_p$	Majority defects change from $(h^{\bullet}, Ca_Y^{'})$ to $(Ca_Y^{'}, V_O^{\bullet\bullet})$ & $(V_O^{\bullet\bullet}, e^{'})$ with decreasing P_{O_2}.
Kim & Yoo[3]	Impedance spectroscopy, DC relaxation and thermoelectric power of as a function of P_{O_2} and T.	—	Majority defects change from $(h^{\bullet}, Ca_Y^{'})$ to $(Ca_Y^{'}, V_O^{\bullet\bullet})$ & $(V_O^{\bullet\bullet}, e^{'})$ with decreasing P_{O_2}. Anti-Frenkel disorder with oxygen interstitials.
Cao *et al*.[4]	DC conductivity and thermoelectric power as a function of P_{O_2} and T; FT-IR, XRD	Disproportionation of Fe^{3+}; n-type: Charge carrier is e' associated with $Fe_{Fe}^{'}(Fe^{2+})$	—
Liu *et al*.[5]	DC conductivity as a function of T in air; XRD, SEM	p-type semiconductor	In air majority defects are $(h^{\bullet}, Ca_Y^{'})$ $CaO + \frac{1}{4}O_2(g) + Y_Y^{X} \rightarrow Ca_Y^{'} + h^{\bullet} + \frac{1}{2}Y_2O_3$

concentrations is $Ca_2Fe_2O_5$ with browmillerite structure, which is an example of perovskite oxide (ABO_3) with ordered anion vacancies. One-sixth of the oxygen ions are missing. The oxygen vacancies are ordered in alternate (001) BO_2 planes of the cubic structure such that alternate [110] rows of oxide ions are missing. Hence, $Y_{1-x}Ca_xFeO_{3-\delta}$ can be considered as a solid solution of $Ca_2Fe_2O_5$ in $YFeO_3$.

Experimental Procedure

Materials

Starting materials used for the preparation of $Y_{1-x}Ca_xFeO_{3-\delta}$ were Y_2O_3, Fe_2O_3 and $CaCO_3$ powders of purity > 99.99%. They were mixed in the appropriate ratio to prepare samples characterized by x = 0.00, 0.025, 0.05 and 0.10. Powders were initially calcined in flowing air at 1200 K for ~ 40 ks. The calcined samples were ground, pressed in steel die at 100 MPa and sintered at 1625 K in air for ~ 60 ks. The sintered samples were 10 mm in diameter and 12.5 mm long. The sintered samples were found to be single phase by XRD and SEM with density 96% of the theoretical value. The mean grain size was 7 μm.

DC electrical conductivity measurements

DC electrical conductivity measurements were performed using 4-probe technique. Separate pairs of current-carrying and voltage-sensing electrodes were used as shown in Fig. 1. For the purpose of illustration an elongated cylindrical sample is shown in the figure showing the relative position of the probes. Platinum paste was applied on top and bottom of the sintered pellet, which was then heat treated at 1200 K for 1.8 ks. Platinum lead wires of 0.4 mm in diameter, pressed against the platinized surfaces, were used as current carrying leads. Potential measurements were made by attaching Pt wires of 0.2 mm diameter at a distance of 2 mm from each platinized surface. A current was passed through

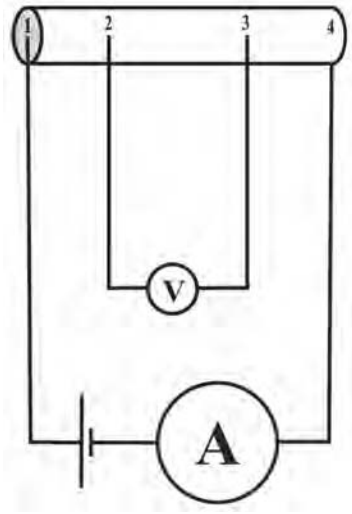

Fig. 1—Schematic diagram of the 4-probe DC conductivity measurement scheme.

the sample using the outer leads, and the inner leads were used for voltage measurement using a high impedance voltmeter. The main advantage of the four-probe method is that the separation of current and voltage electrodes allows the elimination of the resistance contribution of wiring and contacts.

Determination of Seebeck coefficient

Seebeck measurements are useful for identifying the dominant electronic carrier in the material. The thermoelectric power that appears between hot and cold ends of the material is measured. If the potential of the hot end is negative, the predominant charge carriers are holes. Conversely, if the potential of the hot end is positive, the charge carriers are electrons. When both electrons and holes are present, the difference in the number and mobility between electrons and holes determines the sign of the Seebeck coefficient.

A temperature gradient of ~ 20 K across the length of the specimen was imposed using an experimental arrangement shown schematically in Fig. 2. The sample with two end-faces coated with Pt paste was placed inside a furnace for thermo e.m.f. measurement. The temperature differential was achieved by placing the sample on a micro-heater embedded in cast ceramic. The temperature difference (ΔT) between the two ends of the sample was measured using Pt/Pt-13%Rh thermocouples as shown in the figure. The overall temperature of the sample was controlled by the main furnace and the temperature difference was controlled by varying the current through the micro-heater. The thermo e.m.f. developed between the two ends of the sample was measured using a high impedance voltmeter. From the measured thermo e.m.f. and temperature differential, Seebeck coefficient (S) was calculated using the expression

$$S = -\frac{\Delta V}{\Delta T} = \frac{E}{\nabla T} = -\frac{V_{T_2} - V_{T_1}}{T_2 - T_1} \quad \ldots (1)$$

where V is the voltage, E is the electric field and ∇T is temperature gradient.

Results and Discussion

The temperature variation of DC electrical conductivity of $Y_{1-x}Ca_xFeO_{3-\delta}$ in the range from 625 to 1250 K is shown in Fig. 3. All samples exhibit the semiconducting behaviour. Addition of

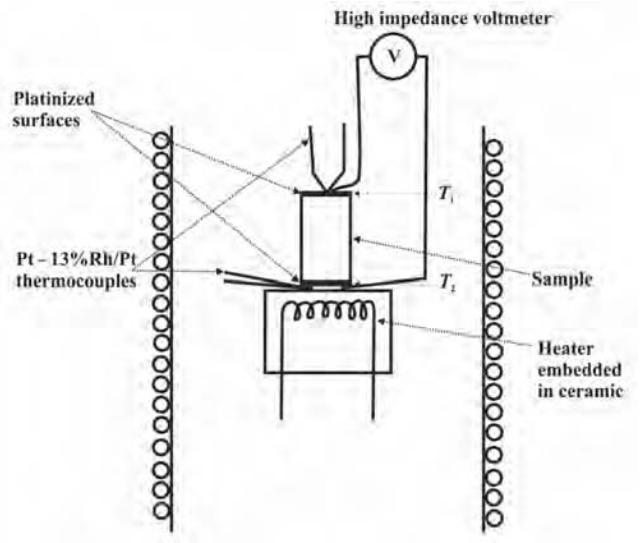

Fig. 2—Schematic diagram of the experimental setup for the determination of Seebeck coefficient.

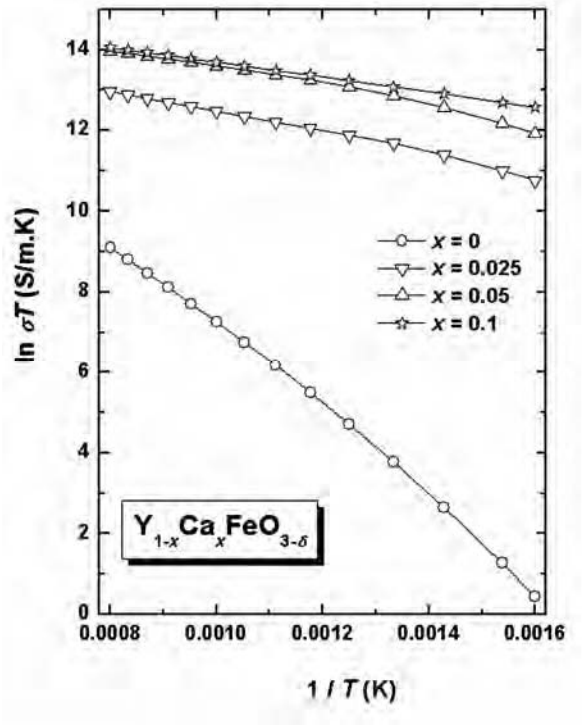

Fig. 3—Arrhenius plots of DC conductivity of $Y_{1-x}Ca_xFeO_{3-\delta}$ for x = 0, 0.025, 0.05 and 0.1.

Ca dramatically increases the conductivity of $YFeO_3$. The plot of $\ln(\sigma T)$ versus reciprocal of absolute temperature is non-linear for all compositions. Nonlinearity persists when $\ln(\sigma T^{3/2})$ is plotted as a function of $1/T$ conforming to the requirement for thermally activated small-polaron mechanism.

Figure 4 shows the compositional variation of DC electrical conductivity at 700 and 1200 K. The effect of Ca in increasing of conductivity decreases with increase in concentration. There is only marginal increase in conductivity when Ca concentration is increased from 5 to 10 mol %. The enhancement of conductivity caused by addition of Ca is more dramatic at the lower temperature.

Activation energy for conduction can be derived from the slope of the curves in Fig. 3 using the formula

$$\frac{\mathrm{d}\left(\ln \sigma T\right)}{\mathrm{d}(1/T)} = \frac{-E_{\mathrm{A}}}{\mathrm{k}} \qquad \ldots (2)$$

where σ is the conductivity at temperature T, E_{A} is the activation energy, k is the Boltzmann constant. The activation energy for conduction of each composition decreases with increasing temperature as shown in Fig. 5. The activation energy decreases continuously from 1.14 to 0.76 eV for pure $YFeO_3$ with increasing temperature. The orthoferrite is known to exhibit a second order magnetic transition from anti-ferromagnetic to para-magnetic around 644.5 K[7]. The change in activation energy may be partly related to this phase transition. The activation energy for sample with x = 0.025 decreases with increase in temperature up to 800 K and then becomes almost independent of temperature within experimental error. For the composition x = 0.05 the activation energy for conduction decreases with increase in temperature up to 1000 K and thereafter becomes almost independent of temperature. The activation energy for conduction for x = 0.1 shows almost temperature-independent behaviour.

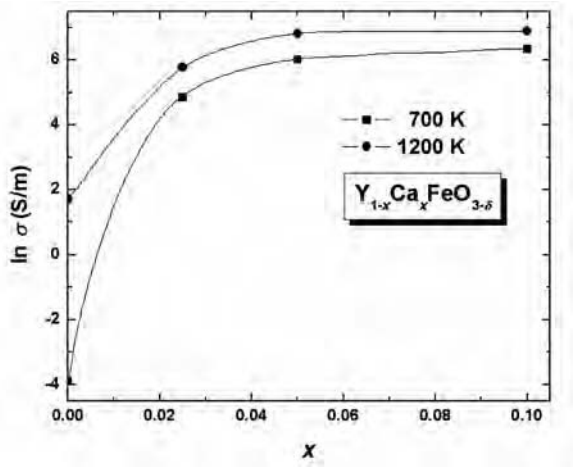

Fig. 4—Variation of DC conductivity of $Y_{1-x}Ca_xFeO_{3-\delta}$ with composition at T = 700 K and 1200 K.

Conductivity results obtained in this study can be compared with the values reported in the literature[2,4,5]. Figure 6 compares temperature dependence of DC electrical conductivity of pure $YFeO_3$. The results obtained in the study agree with the values of Cao *et al*.[4] The results of Liu *et al*.[5] show a weaker temperature dependence; their values are significantly lower at higher temperatures and higher at lower

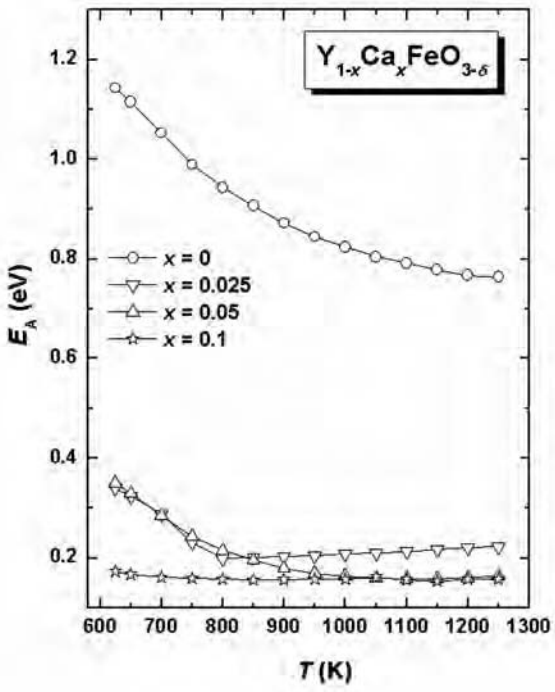

Fig. 5—Variation of activation energy for electrical conduction in $Y_{1-x}Ca_xFeO_{3-\delta}$ with x = 0, 0.025, 0.05 and 0.1 as a function of temperature.

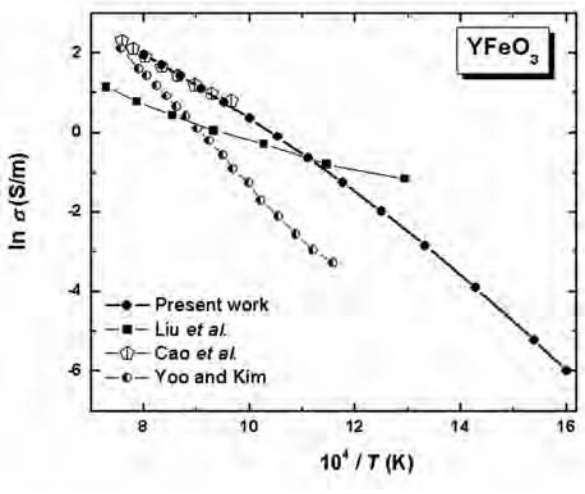

Fig. 6—Comparison of electrical conductivity of pure $YFeO_3$ obtained in different studies.

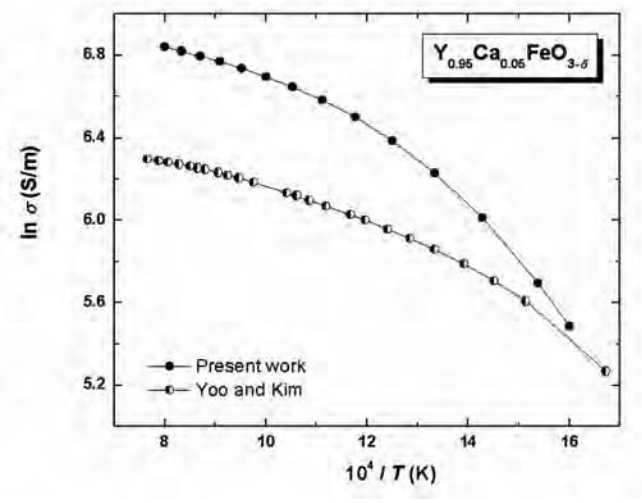

Fig. 7—Comparison of electrical conductivity of $Y_{0.95}Ca_{0.05}FeO_{3-\delta}$ obtained in this study with that reported by Yoo and Kim[2]

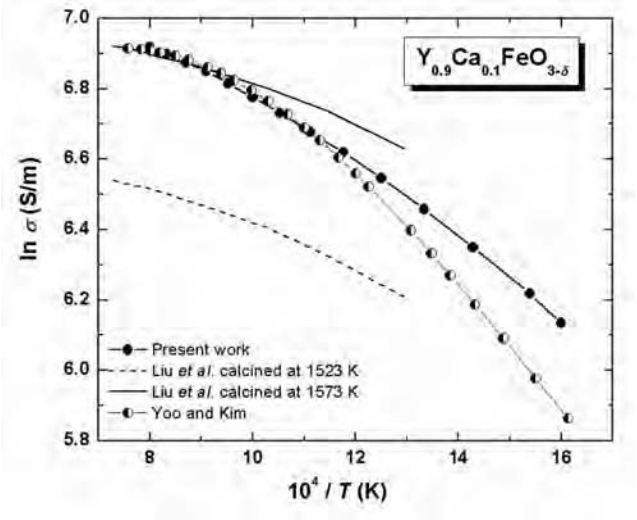

Fig. 8—Comparison of electrical conductivity of $Y_{0.9}Ca_{0.1}FeO_{3-\delta}$ obtained in different studies.

temperatures than results obtained in this study, with data crossover at ~ 900 K. The results of Yoo and Kim[2] show a stronger temperature dependence of conductivity; their values are significantly lower at lower temperatures, but approach values obtained in this study near 1200 K.

Figure 7 shows that the temperature dependence of DC electrical conductivity for the composition with x = 0.05; the conductivity measured in this study is significantly higher than the values reported by Yoo and Kim [2] at higher temperatures, but both data sets appear to converge at lower temperatures. The electrical conductivity of the composition x = 0.1 obtained in this study agrees with previous measurements[2,5] at high temperatures as shown in Fig. 8, and falls between previous studies[2,5] at lower temperatures. The data of Liu *et al.*[5] on porous gelcast samples is dependent on sintering temperature. The conductivity of samples sintered at lower temperature is significantly reduced because of higher porosity.

The measured Seebeck coefficients are summarized in Table 2. Seebeck coeffient in air was found to be positive indicating *p*-type material with positively charged carriers (holes). The value of Seebeck coefficient for pure $YFeO_3$ showed temperature dependence, decreasing from 440(±20) μV/K at 1150 K to 390(±20) μV/K at 1350 K. For $Y_{1-x}Ca_xFeO_{3-\delta}$ with x = 0.025, the Seebeck coefficient exhibited a constant value of 415(±20) μV/K independent of temperature. The results obtained in this study are consistent with the measurements of Yoo and Kim[2] and Kim and Yoo[3], but are contrary

Table 2—Measured Seebeck coefficients of $Y_{1-x}Ca_xFeO_{3-\delta}$ in air

Composition	Seebeck coefficient, θ / mV·K^{-1}		
	1150 K	1250 K	1350 K
$YFeO_3$	440 (±20)	420 (±20)	390 (±20)
$Y_{0.975}Ca_{0.025}FeO_{3-\delta}$	410 (±20)	405 (±20)	415 (±20)

to the findings of Cao *et al.*[4] Since the study of Cao *et al.*[4] involved many samples of $YFe_{1-y}Mn_yO_3$, it is likely that their sample of pure $YFeO_3$ was contaminated by Mn refluxing from the refractory lining of the furnace.

It is useful to visualize the conductivity behaviour on the basis of defect chemistry. In undoped $YFeO_3$, the charge carriers in air are probably of intrinsic origin (nil = e' + h$^\bullet$) generated by the disproportionation of Fe^{3+} as suggested by Yoo and Kim[2]:

$$2Fe^{x}_{Fe} \rightarrow Fe^{\bullet}_{Fe} + Fe^{'}_{Fe} \quad \ldots (3)$$

where Kröger-Vink notation is used to represent defects. Thus, $Fe^{'}_{Fe}$ represents Fe^{2+} ion with an electron localized on Fe^{3+} on its normal lattice site, and $Fe^{\bullet}_{Fe}$ represents Fe^{4+} ion with a hole localized on Fe^{3+}. Positive value of the Seebeck coefficient indicates that hole mobility is significantly higher than electron mobility. At low concentrations, the substitution of Ca^{2+} for Y^{3+} in $YFeO_3$ is electronically compensated by the formation of Fe^{4+} or $Fe^{\bullet}_{Fe}$.

$$xCaFeO_{2.5} + 1/4O_2 \rightarrow xCa^{'}_{Y} + xFe^{\bullet}_{Fe} + 3xO^{x}_{O} \quad \ldots (4)$$

where Ca'_Y is a Ca^{2+} cation on Y^{3+} lattice position with an effective negative charge and O^x_O is a O^{2-} anion on a regular site with no effective charge. Although there is no direct evidence of Fe^{4+} ion, the existence of compounds such as $SrFeO_3$ indicates that Fe^{4+} ion can be stabilized in ternary oxides under suitable conditions. The electro-neutrality condition is

$$\left[Ca'_Y\right]=\left[Fe^{\bullet}_{Fe}\right]=\left[h^{\bullet}\right] \quad \ldots (5)$$

where the square brackets represent the concentration of species within them. Charge compensation for Ca on the A-site by the formation of Fe^{4+} on the B-site is energetically more favourable than the formation of oxygen vacancies at low Ca concentrations. The entropy factor also favours Fe^{4+} defects since more defects are created by this process than by the oxygen vacancy mechanism. In this defect domain, conductivity will increase significantly with concentration of Ca and be independent of oxygen partial pressure at constant composition as observed in this study (Fig. 4) and by Yoo and Kim[2] and Kim and Yoo[3]. Conduction mechanism involves the hopping of holes between Fe^{4+} and Fe^{3+} on the regular site.

Based on the variation of ionic conductivity with partial pressure, Kim and Yoo[3] suggested the predominance of oxygen interstitials at high oxygen partial pressure. In view of the relatively limited accuracy of ionic conductivity and electro-transport measurements, this conclusion is perhaps overdrawn. Introduction of interstitial oxygen in perovskite structure is thermodynamically unfavourable.

Electrostatic repulsion between Fe^{4+} ions can tilt the balance towards oxygen vacancies as the charge compensating mechanism at higher values of x. At relatively low partial pressures of oxygen, high concentration of Ca and at high temperatures, there is a tendency for oxygen vacancy formation and this happens by the partial reduction of Fe^{4+} cation to Fe^{3+}.

$$2Fe^{\bullet}_{Fe}+O^x_O \rightarrow 2Fe^x_{Fe}+V^{\bullet\bullet}_O+1/2\,O_2 \quad \ldots (6)$$

where $V^{\bullet\bullet}_O$ represents oxygen ion vacancy on anionic sublattice with two effective positive charges. Thus, hole conductivity decreases with decreasing partial pressure of oxygen:

$$2\left[Fe^{\bullet}_{Fe}\right]=\left[h^{\bullet}\right]\propto P_{O_2}^{1/4} \quad \ldots (7)$$

The electro-neutrality condition is given by,

$$\left[Ca'_Y\right]=\left[Fe^{\bullet}_{Fe}\right]+2\left[V^{\bullet\bullet}_O\right] \quad \ldots (8)$$

The more gradual increase in conductivity with concentration at higher Ca content (Fig. 4) is indicative of the gradual shift in the charge compensation from $Fe^{\bullet}_{Fe}$ to $V^{\bullet\bullet}_O$.

At sufficiently low oxygen partial pressures, when all the Fe^{4+} ions have been consumed, the defect reaction becomes,

$$O^x_O \rightarrow 1/2\,O_2+2Fe'_{Fe}+V^{\bullet\bullet}_O \quad \ldots (9)$$

The conductivity will therefore change from *p*-type to *n*-type at very low oxygen partial pressures according to the relation,

$$\left[Fe'_{Fe}\right]=\left[e'\right]\propto P_{O_2}^{-1/4} \quad \ldots (10)$$

Evidence for such a change in the nature of conduction is provided by the conductivity and Seebeck measurements of Yoo and Kim[2]. Conduction occurs by the hopping of electrons between Fe^{2+} and Fe^{3+} ions. The electro-neutrality condition for this case is:

$$\left[Ca'_Y\right]+\left[Fe'_{Fe}\right]=\left[V^{\bullet\bullet}_O\right] \quad \ldots (11)$$

The small ($<10^{-2}$) but increasing oxygen ion transport number with decreasing oxygen partial pressure in $Y_{0.9}Ca_{0.1}FeO_{3-\delta}$ in the temperature range from 1173 to 1373 K observed by Kim and Yoo[3] supports the formation of oxygen vacancies at reduced oxygen chemical potentials.

Conclusions

DC electrical conductivity of the solid solution $Y_{1-x}Ca_xFeO_{3-\delta}$ with x = 0.0, 0.025, 0.05 and 0.1 was studied in the temperature range from 625 to 1250 K. All $Y_{1-x}Ca_xFeO_{3-\delta}$ samples showed semiconducting behaviour. Seebeck coefficient in air was found to be positive indicating *p*-type conduction. A dramatic increase in the conductivity of $YFeO_3$ with small additions of CaO was observed. This is related to the formation of holes localized on Fe^{3+} ions on their regular lattice sites to charge compensate for Ca^{2+} ions on the Y^{3+} sites. With increase in the concentration of Ca, the charge compensating mechanism shifts from electron holes to oxygen vacancies. Consequently, electrical conductivity shows only marginal increase beyond x = 0.05. With decrease in oxygen partial pressure, the conductivity remains almost constant

initially and then decreases. At a low oxygen partial pressure, *p*-type conductivity changes to *n*-type. Further reduction in oxygen partial pressure results in an increase in conductivity. The results obtained in this study confirm the results of Yoo and Kim[2] for $Y_{1-x}Ca_xFeO_{3-\delta}$, but disagree with the observations of Cao *et al*.[4] for pure $YFeO_3$.

Acknowledgements

K T Jacob is grateful to the Indian National Academy of Engineering, New Delhi, for the award of INAE Distinguished Professorship. G Rajitha thanks the University Grants Commission, New Delhi, India for the award of Dr D S Kothari Postdoctoral Fellowship.

References

1 Wyckoff R W G, *Cyrstal Structures*, (Interscience Publishers, New York), 1964.
2 Yoo H I & Kim C S, *Solid State Ionics*, 53-56 (1992) 583.
3 Kim C S & Yoo H I, *J Electrochem Soc*, 143 (1996) 2863.
4 Cao X, Kim C S & Yoo H I, *J Am Ceram Soc*, 84 (2001) 1265.
5 Liu X, Gao J, Liu Y, Peng R, Peng D & Meng G, *Solid State Ionics*, 152-153 (2002) 531.
6 Jacob K T, Dasgupta N & Vineeth P R, *J Phase Equilib Diffus*, (2010) accepted for publication
7 Shen H, Xu J, Wu A, Zhao J & Shi M, *Mater Sci Eng B*, 157 (2009) 77.